

Introducing vortices in the continuum using direct and indirect methods

Zahra Asmaee* and Sedigheh Deldar†
*Department of Physics, University of Tehran,
P. O. Box 14395/547, Tehran 1439955961, Iran*

Motahareh Kiamari‡
*School of Particles and Accelerators, IPM,
P. O. Box 19395-5531, Tehran, Iran*

Inspired by direct and indirect maximal center gauge methods which confirm the existence of vortices in lattice calculations and by using the connection formalism, we show that under some appropriate gauge transformations vortices and chains appear in the QCD vacuum of the continuum limit. In the direct method, by applying center gauge transformation and “center projection,” QCD is reduced to a gauge theory including vortices, which corresponds to the non-trivial first homotopy group $\Pi_1(\text{SO}(3)) = Z_2$. On the other hand, using the indirect method, in addition to the center gauge transformation and “center projection,” an initial step called Abelian gauge transformation and then Abelian projection are applied. Therefore, instead of single vortices, chains that contain monopoles and vortices appear in the theory.

PACS numbers: 12.38.Aw, 12.38.Lg, 12.40.-y.

I. INTRODUCTION

Quantum chromodynamics is the non-Abelian gauge theory of the strong interaction which describes the hadrons in terms of quarks and gluons. There are many books that discuss QCD; for instance, see Refs. [1, 2]. However, quarks have not been observed as isolated particles in the real world. Only hadrons (mesons and baryons) are observed as some color singlet combinations. This experimental fact reflects the confinement mechanism as one of the most controversial unsolved issues in particle physics in the low-energy regime or large distances [3, 4]. During the past decades, many ideas have been proposed to approach this problem. There are many articles about this subject; for instance, see Refs. [5–11].

The area law of the Wilson loop average is a well-known gauge-invariant criterion in studying quark confinement. It leads to a linear potential between a pair of static quark-antiquark. To study the linear part of the confinement potential, the quenched approximation is used where the dynamical quarks are removed for the infrared regime [4]. In fact, one can obtain some collective modes from gluons [12] which are associated with some topological degrees of freedom of the QCD vacuum, and as a result it is assumed that the QCD vacuum is filled with the topological objects obtained from these collective modes. Magnetic monopoles and center vortices are among the main candidates for describing confinement and each has its own fans.

For the non-perturbative description, people use lattice QCD simulations and phenomenological models to look

for the confinement and topological objects. The results of the phenomenological models must be in agreement with the results of the lattice QCD, though. In fact, lattice QCD can be served as a laboratory for confirming the correctness or incorrectness of the phenomenological models.

In the absence of matter fields, some various mechanisms of confinement have been suggested to extract the topological degrees of freedom of pure Yang-Mills theory. One of those mechanisms is the picture of the dual superconductor and appearance of Abelian monopoles. It was proposed by Nambu [13], Mandelstam [14], 't Hooft [15] and Polyakov [16] in the 1970s. The idea is that the QCD vacuum can behave like a dual superconductor and it is filled with magnetic monopoles. Just as the Meissner effect leads to the condensation of the Cooper pairs as electrically charged objects in an ordinary superconductor, the magnetic monopoles are condensed in a dual superconductor and squeeze the chromoelectric flux between the quark-antiquark pair inside a tube. Therefore, confinement of electric fields is obtained as a result of the condensation of magnetic monopoles in this picture [12, 17, 18].

The second possible mechanism is given by the center vortex model [19–25]. Historically, vortex-like structures were introduced in superconductors in 1959. Even though they were not observed at that time, they were recognized a few years later by Abrikosov [26]. It was proposed in various forms by 't Hooft [27–30], Nielsen and Olesen [31], Ambjorn and Olesen [32], Mack and Petkova [33, 34], and Cornwall [35] in the late 1970s with a field theoretical approach. The idea is that the QCD vacuum is filled with closed magnetic vortices, and it is assumed that the vortices are condensed in the QCD vacuum. If a Wilson loop is linked to a vortex in an $\text{SU}(N)$ gauge group, the Wilson loop obtains a phase difference equal to $e^{i2\pi n/N}$ ($n = 0$ to $N - 1$) corresponding to the type of

* zahra.asmaee@ut.ac.ir

† sdeldar@ut.ac.ir

‡ mkiamari@ipm.ir

the vortex. As a result, some disorders are created in the lattice which eventually lead to an area law fall-off and confinement.

Vortices are defined by the center of the $SU(N)$ gauge group and there exist $(N - 1)$ distinct vortices, which are called non-Abelian Z_N vortices. The simplest vortices are defined by the Z_2 gauge group and they have the topology of tubes (in three Euclidean dimensions) or surfaces of finite thickness (in four dimensions) carrying some well-defined magnetic fluxes [5, 27, 28, 31–35].

Lattice calculations show that Z_N vortices produce full string tensions as the Yang-Mills vacuum does. This is an encouraging motivation to study confinement via center vortices. If the center vortices are removed from the lattice, the string tension also disappears [19, 21, 23, 36–38].

The vortex condensation picture relies upon center gauge fixing and center projection. After performing center projection in lattice QCD, the full QCD with $SU(N)$ gauge symmetry is reduced to a gauge theory with a $Z(N)$ gauge symmetry. These vortices are called projection vortices (or p-vortices). Unlike monopoles, the modified models of vortices like thick center vortices can qualitatively explain the Casimir scaling dependence for all representations [20].

To study the confinement problem by center vortices, one first has to discuss the existence of vortices in the continuum limit. The most common methods of identifying vortices in the lattice simulation are direct maximal center gauge (DMCG) [21] and indirect maximal center gauge (IMCG) [19]. Inspired by these two methods of identifying vortices in lattice calculations and by the help of the connection formalism [12], we discuss the appearance of vortices in the continuum limit of QCD.

We review DMCG and IMCG methods in lattice QCD in Sec. II. In Sec. III, motivated by the methods proposed in lattice calculations, we introduce the vortices in the continuum by direct method for $SU(N)$ gauge group. As an example, by applying an appropriate gauge transformation in the $SU(2)$ gauge group and using the results of Sec. III, we show in Sec. IV that under the center gauge transformation the vortex and anti-vortex can appear in the theory. Then, we remove the term that represents the anti-vortex. The theory has an $SO(3)$ symmetry containing the vortex, which corresponds to the non-trivial first homotopy group of $\Pi_1(SO(3)) = Z_2$. Removal of the contribution of the anti-vortex is called “center projection” in our paper. In Sec. V, we introduce thin vortices in the continuum by the indirect method for $SU(N)$ gauge group. Sec. VI is brought in two subsections. In Sec. VIA, applying an Abelian gauge transformation for $SU(2)$ gauge theory, we show that the QCD vacuum is filled with monopoles and anti-monopoles. It is shown that after Abelian projection the monopole appears in the vacuum and the gauge group symmetry is reduced from $SU(2)$ to $U(1)$ and we have a monopole vacuum. Then, in Sec. VIB we show that under a center gauge transformation on the monopole vacuum the

vortex and anti-vortex appear in the gauge theory along with the monopole. After applying a “center projection” we have a gauge theory that contains chains including monopoles and vortices.

II. DMCG AND IMCG IN LATTICE QCD

There are some methods to identify vortices in lattice calculations and by using appropriate gauge transformations, which are in agreement with the vortex condensation picture [19–21, 23, 24].

In lattice QCD, the action is expressed in terms of link variables on which the gluon fields are defined. The idea is that under an appropriate gauge transformation the link variables $U_\mu(x)$ get as close as possible to the center gauge group; center $(SU(N)) = Z_N$. Then, after a projection, a smaller set of degrees of freedom remains. This job is usually done via two methods in lattice QCD calculation. In the following, we briefly review both methods.

A. Direct maximal center gauge method

This method was proposed by Del Debbio *et al.* [21], who tried to maximize the following quantity by determining the gauge transformation $G(x) \in SU(N)$:

$$R[U] = \max_G \sum_{x,\mu} |\text{Tr } U_\mu^G(x)|^2. \quad (1)$$

$U_\mu^G(x) = G(x)U_\mu(x)G^\dagger(x + \hat{\mu})$ shows the gauge transformation of the link variables $U_\mu(x)$ and as a result of the above maximization, U_μ^G becomes as close as possible to the center elements. $\hat{\mu}$ is a unit vector along the μ direction. Then, by performing the center projection, one replaces the transformed link variable $U_\mu^G(x)$ by the closest associated center elements of the group Z_N . As an example, the center projection is defined for the $SU(2)$ gauge group as

$$U_\mu^G(x) \rightarrow Z(2) = \text{sign} [\text{Tr } U_\mu^G(x)] \mathbf{1} = \{+1, -1\} \times \mathbf{1}, \quad (2)$$

where $\mathbf{1}$ represents a 2×2 unit matrix. P-vortices identified by the DMCG method, are related to the non-perturbative degrees of freedom; see Ref. [4] for more details.

B. Indirect maximal center gauge method

The indirect maximal center gauge method was originally examined in lattice QCD for the $SU(2)$ gauge group [19]. In general, for an $SU(N)$ gauge group, the procedure is as the follows. For the first step, a non-Abelian gauge configuration is fixed under Abelian gauge fixing, and after Abelian projection, the $SU(N)$ gauge symmetry

is reduced to $[U(1)]^{N-1}$. In the second step, the remaining $[U(1)]^{N-1}$ configuration is fixed under center gauge fixing such that the transformed gauge fields become as close as possible to the center elements. Finally, by performing a center projection, one gets the center elements. For example, for the $SU(2)$ gauge group,

$$Z(2) = \sum_{x,\mu} \text{sign}[\cos\theta(x,\mu)] \mathbf{1} = \{+1, -1\} \times \mathbf{1}, \quad (3)$$

where $\theta(x,\mu)$ parametrizes the links. In general, in both methods, identification of the vortices is done by using gauge fixing and then projection.

III. DIRECT METHOD OF INTRODUCING VORTICES IN THE CONTINUUM

In this section, inspired by DMCG method in lattice QCD which confirms the existence of vortices in the infrared regime, we show that vortices appear in the theory by a singular gauge transformation. In this procedure, we use the connection formalism, which is applied for the singular gauge transformation. We would like to mention that we do not find a continuum formula for maximal center gauge transformation, Eq.(1), which has already been done in Ref. [39]. Instead, motivated by the fact that vortices exist in the infrared part of the theory, as shown by the lattice calculations, we use the connection formalism to make explicit the vortices, somehow similar to the procedure done in Ref. [12] for monopoles.

A. Link variable and transformed gluon field

In lattice gauge theory, color confinement can be studied by quenched approximation where only gluon fields exist in the theory. Gluons are defined on link variables as follows:

$$U_\mu(x) = e^{iagA_\mu(x)} \in SU(N). \quad (4)$$

Under a gauge transformation $G(x) \in SU(N)$, the link variables are transformed as

$$U_\mu(x) \rightarrow U_\mu^G(x) = G(x)U_\mu(x)G^\dagger(x + \hat{\mu}). \quad (5)$$

Using Eq.(4) in the above equation,

$$U_\mu^G(x) = G(x)e^{iagA_\mu(x)}G^\dagger(x + \hat{\mu}). \quad (6)$$

Since the lattice spacing a is small enough, we can use the exponential expansion of $e^{iagA_\mu(x)}$, and using the Taylor expansion for $G^\dagger(x + \hat{\mu})$,

$$\begin{aligned} U_\mu^G &= 1 + iag \left[G(x)A_\mu G^\dagger(x) - \frac{i}{g}G(x)\partial_\mu G^\dagger(x) \right] + \mathcal{O}(a^2) \\ &= e^{iagA_\mu^G}. \end{aligned} \quad (7)$$

Thus, in the continuum limit where $a \rightarrow 0$, the gluon field is transformed as

$$A_\mu^G(x) = G(x)A_\mu(x)G^\dagger(x) - \frac{i}{g}G(x)\partial_\mu G^\dagger(x), \quad (8)$$

where $A_\mu^G(x) \in SU(N)$. In terms of group generators,

$$\vec{A}_\mu^G \cdot \vec{T} = G(x) (A_\mu^c T^c) G^\dagger(x) - \frac{i}{g}G(x)\partial_\mu G^\dagger(x), \quad (9)$$

T^c are generators of the $SU(N)$ group, and c is the color index.

Since we are interested in observing topological defects from the gluon fields, we have to use an appropriate gauge transformation. Thin vortices appear as topological defects after center gauge transformations and some subsequent efforts.

Equation (9) can be used to study the vortices if $G(x) \equiv N(x)$ is defined as a center gauge transformation,

$$\vec{A}_\mu^N \cdot \vec{T} = N(x) (A_\mu^c T^c) N^\dagger(x) - \frac{i}{g}N(x)\partial_\mu N^\dagger(x). \quad (10)$$

To study the contribution of thin vortices in the continuum, we first recall that in lattice QCD calculations when the Wilson loop links to the vortex it receives a phase difference equal to $e^{i2\pi n/N}$ associated with the non-trivial center element contribution $Z(k)$ [18],

$$W(C) \rightarrow e^{i2\pi n/N} W(C), \quad (n = 1, 2, \dots, N-1). \quad (11)$$

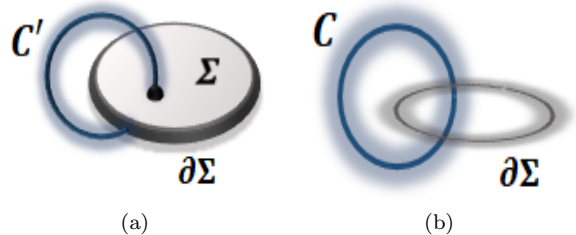


FIG. 1: Linking between the Wilson loop C and a vortex with hypersurface Σ . The boundary of the hypersurface is shown by $\partial\Sigma$, indicating a thin vortex.

Under a center gauge transformation $N(x)$, a Wilson line should be transformed as

$$\begin{aligned} W(C') &\rightarrow W^N(C') = N(x - \epsilon)W(C')N^\dagger(x + \epsilon) \\ &= N(x - \epsilon)N^\dagger(x + \epsilon) + \mathcal{O}(\epsilon) \quad (12) \\ &\equiv Z(k) + \mathcal{O}(\epsilon), \end{aligned}$$

$W(C') = 1 + \mathcal{O}(\epsilon)$. C' indicates an open circle from $x - \epsilon$ to $x + \epsilon$, where x indicates the location of the intersection of C' and the hypersurface Σ . ϵ is an infinitesimal quantity so that in the limit where $\epsilon \rightarrow 0$, $C' = C$.

We use Eq.(12) to obtain the appropriate gauge transformation $N(x)$, which gives the non-trivial center elements indicating the existence of vortices in the last line of Eq.(12).

From Fig. 1(a), an ideal vortex is defined on $(D - 1)$ -dimensional hypersurface Σ , while the thin vortex is defined on $(D - 2)$ -dimensional boundary $S = \partial\Sigma$ [18, 39]. Piercing the hypersurface by the Wilson loop results in a discontinuity $Z(k)$. The center vortex in $D = 2, 3$, and 4 is defined as a string, surface, and volume, respectively.

The relation between an ideal vortex and a thin vortex is as follows [18, 39]:

$$\text{ideal vortex} = -\frac{i}{g}N(x)\partial_\mu N^\dagger(x) - \text{thin vortex}. \quad (13)$$

In fact, intersecting the hypersurface Σ of an ideal vortex with a Wilson loop C gives a phase to the Wilson loop proportional to a center group element. The boundary $\partial\Sigma$ indicates the location of the thin vortex, which is gauge equivalent to the ideal vortex. Thus, the ideal vortex field is not unique and can be gauge transformed to a thin vortex field which has the support only on the boundary $\partial\Sigma$ [18].

Replacing $\left(-\frac{i}{g}N(x)\partial_\mu N^\dagger(x)\right)$ from Eq.(13) in Eq.(10),

$$\vec{A}_\mu^N \cdot \vec{T} = N(x) (A_\mu^c T^c) N^\dagger(x) + \text{ideal vortex} + \text{thin vortex}. \quad (14)$$

On the other hand, in analogy to the lattice calculation where the thin vortex links to the Wilson loop [Fig.1(b)], one can define a gauge field in the coset space by removing the ideal vortex [39] so that $\vec{A}_\mu^N \cdot \vec{T} \rightarrow \vec{A}'_\mu \cdot \vec{T}$;

$$\vec{A}'_\mu \cdot \vec{T} = N(x) (A_\mu^c T^c) N^\dagger(x) + \text{thin vortex}. \quad (15)$$

We recall that $\vec{A}'_\mu \cdot \vec{T}$ is still singular on $\partial\Sigma$. The gauge field configuration $\vec{A}'_\mu \cdot \vec{T}$ induces the same behavior for arbitrary Wilson loop as the configuration $\vec{A}_\mu^N \cdot \vec{T}$ does. In other words, for $x \notin$ hypersurface, we only see the boundary of the vortex, called the thin vortex field. In fact, by this choice of x , we have removed the hypersurface Σ from the space-time. So, the contribution of the ideal vortex defined on the hypersurface vortex would be zero;

$$\text{thin vortex} = -\frac{i}{g}N(x)\partial_\mu N^\dagger(x), \quad x \notin \text{hypersurface}. \quad (16)$$

B. Field strength tensor and connection formalism

In this subsection, we discuss the connection formalism, which has already been used in some references, for instance, Refs. [12, 40]. In fact, we generalize the connection formalism, previously applied to the Abelian gauge transformation, to the center gauge transformation.

The Yang-Mills Lagrangian has an $SU(N)$ symmetry and is given by

$$\mathcal{L}_{\text{YM}} = -\frac{1}{2}\text{Tr}(F_{\mu\nu}F^{\mu\nu}), \quad (17)$$

where the $SU(N)$ non-Abelian field strength tensor called $F_{\mu\nu} = \vec{F}_{\mu\nu} \cdot \vec{T} = F_{\mu\nu}^c T^c$ is defined by $F_{\mu\nu} = \partial_\mu A_\nu - \partial_\nu A_\mu + ig[A_\mu, A_\nu]$ and for a regular system can be written as

$$F_{\mu\nu} = \frac{1}{ig} [\hat{D}_\mu, \hat{D}_\nu], \quad \hat{D}_\mu = \partial_\mu + igA_\mu, \quad (18)$$

where \hat{D}_μ is the covariant-derivative operator.

But topological defects appear as a result of singular gauge transformation. To observe these defects explicitly, we rewrite the Yang-Mills gauge theory in terms of the covariant-derivative operator D_μ and the ordinary derivative operator $\hat{\partial}_\mu$,

$$\begin{aligned} \frac{1}{ig} [\hat{D}_\mu, \hat{D}_\nu] &= \frac{1}{ig} [\hat{\partial}_\mu + igA_\mu, \hat{\partial}_\nu + igA_\nu] \\ &= \frac{1}{ig} [\hat{\partial}_\mu, \hat{\partial}_\nu] + [\hat{\partial}_\mu, A_\nu] + [A_\mu, \hat{\partial}_\nu] \\ &\quad + ig[A_\mu, A_\nu]. \end{aligned} \quad (19)$$

Using the $[\hat{\partial}_\mu, f] = \partial_\mu f$,

$$\frac{1}{ig} [\hat{D}_\mu, \hat{D}_\nu] = \frac{1}{ig} [\hat{\partial}_\mu, \hat{\partial}_\nu] + \partial_\mu A_\nu - \partial_\nu A_\mu + ig[A_\mu, A_\nu]. \quad (20)$$

For regular systems, the first term on the right-hand side of Eq.(20) is zero, so we have Eq.(18). But this term is not zero for singular systems. Therefore,

$$F_{\mu\nu} = \frac{1}{ig} [\hat{D}_\mu, \hat{D}_\nu] - \frac{1}{ig} [\hat{\partial}_\mu, \hat{\partial}_\nu], \quad (21)$$

where $F_{\mu\nu}$ is the $SU(N)$ non-Abelian field strength tensor, and Eq.(21) is applied when the singularity exists in the system. As a result of singular gauge transformation, topological defects like monopoles and vortices appear in the theory.

We study the behavior of the non-Abelian field strength tensor under singular gauge transformations.

In general, if $G(x) \in SU(N)$ represents a regular gauge transformation, the field strength tensor is transformed as $F_{\mu\nu}^G = G(x)F_{\mu\nu}G^\dagger(x)$. Therefore, $F_{\mu\nu}$ is

$$\begin{aligned} F_{\mu\nu}^G &= G(x) \{ \partial_\mu A_\nu - \partial_\nu A_\mu + ig[A_\mu, A_\nu] \} G^\dagger(x) \\ &= (\partial_\mu A_\nu^G - \partial_\nu A_\mu^G) + ig[A_\mu^G, A_\nu^G]. \end{aligned} \quad (22)$$

On the other hand, for a singular system where $F_{\mu\nu}$ is defined by Eq.(21), one gets

$$\begin{aligned} F_{\mu\nu}^G &= \frac{1}{ig} G(x) [\hat{D}_\mu, \hat{D}_\nu] G^\dagger(x) - \frac{1}{ig} G(x) [\hat{\partial}_\mu, \hat{\partial}_\nu] G^\dagger(x) \\ &= \frac{1}{ig} [\hat{D}_\mu^G, \hat{D}_\nu^G] - \frac{1}{ig} G(x) [\hat{\partial}_\mu, \hat{\partial}_\nu] G^\dagger(x), \end{aligned} \quad (23)$$

where $\hat{D}_\mu^G = G(x)\hat{D}_\mu G^\dagger(x)$. The first term of Eq.(23) can be written by the help of Eq.(20) for a gauge transformed field,

$$\frac{1}{ig} [\hat{D}_\mu^G, \hat{D}_\nu^G] = \frac{1}{ig} [\hat{\partial}_\mu, \hat{\partial}_\nu] + \partial_\mu A_\nu^G - \partial_\nu A_\mu^G + ig [A_\mu^G, A_\nu^G]. \quad (24)$$

Replacing Eq.(24) in Eq.(23),

$$F_{\mu\nu}^G = (\partial_\mu A_\nu^G - \partial_\nu A_\mu^G) + ig [A_\mu^G, A_\nu^G] + \frac{i}{g} G [\partial_\mu, \partial_\nu] G^\dagger. \quad (25)$$

This is a noticeable result. The last term of Eq.(25) shows the difference between this equation and Eq.(22).

The advantage of using the connection formalism technique is that the gauge theory will remain gauge invariant after the singular gauge transformation. Equation (25) is valid for both the Abelian and center gauge transformations. It has already been discussed for the Abelian gauge transformation [12, 40] and we intend to use it for the center gauge transformation, as well.

If one uses Eq.(25) without applying any projection, a full QCD will be obtained at the end. We discuss how we perform ‘‘center projection’’ in Sec. IV.

IV. DIRECT METHOD FOR INTRODUCING VORTICES IN SU(2) GAUGE GROUP

The formation of center vortices in the QCD vacuum relies upon two steps: center gauge transformation and ‘‘center projection’’. Using the results of Sec. III, we discuss these two steps for the SU(2) gauge group.

Step 1: Center gauge transformation In general, a 2×2 gauge transformation $G(x) \in \text{SU}(2)$ is written in terms of three Euler angles α, β, γ ,

$$G(x) = e^{i\gamma(x)T^3} e^{i\beta(x)T^2} e^{i\alpha(x)T^3} \\ = \begin{pmatrix} e^{\frac{i}{2}[\gamma(x)+\alpha(x)]} \cos \frac{\beta(x)}{2} & e^{\frac{i}{2}[\gamma(x)-\alpha(x)]} \sin \frac{\beta(x)}{2} \\ -e^{-\frac{i}{2}[\gamma(x)-\alpha(x)]} \sin \frac{\beta(x)}{2} & e^{-\frac{i}{2}[\gamma(x)+\alpha(x)]} \cos \frac{\beta(x)}{2} \end{pmatrix} \\ \alpha(x) \in [0, 2\pi), \beta(x) \in [0, \pi], \gamma(x) \in [0, 2\pi), T^c = \frac{\sigma^c}{2}, \quad (26)$$

where T^c 's are generators of the SU(2) group and σ^c 's are Pauli matrices. The center gauge transformation $G(x) \equiv N(x) \in \text{SU}(2)$ is continuous everywhere except at the hypersurface of the vortex. Therefore, the Euler angles are selected in a way that the constraint of Eq.(12) is satisfied. There are different choices for the angles. One

can choose $\alpha = \gamma = \frac{\varphi}{2}$ and $\beta = 0$,

$$N = \begin{pmatrix} e^{i\frac{\varphi}{2}} & 0 \\ 0 & e^{-i\frac{\varphi}{2}} \end{pmatrix}, \quad \varphi \in [0, 2\pi). \quad (27)$$

It can be shown that

$$N(\varphi = \epsilon)N^\dagger(\varphi = 2\pi - \epsilon) = -\mathbf{1}_{2 \times 2} \in Z(2), \quad \epsilon \rightarrow 0, \quad (28)$$

where $(-\mathbf{1}_{2 \times 2})$ represents the non-trivial contribution of the Z(2) gauge group. Thus, the contribution of an ideal vortex is observed at $\varphi = 0$. On the other hand, outside the hypersurface, the contribution of the thin vortex is represented by a pure gauge shown in Eq.(16),

$$\text{thin vortex} \equiv \vec{V}_\mu \cdot \vec{T} = -\frac{i}{g} N \partial_\mu N^\dagger = -\frac{1}{g} \partial_\mu \varphi T^3. \quad (29)$$

The spatial component of thin vortex is

$$\vec{V}_\varphi \cdot \vec{T} = -\frac{g^{-1}}{\rho} T^3, \quad \vec{V}_\rho \cdot \vec{T} = 0. \quad (30)$$

Equation (30) represents the gauge field associated with the thin vortex in cylindrical coordinates. The thin vortex is observed at $\rho = 0$ [39] in the third direction of color space. Under a center gauge transformation, the gluon field is defined by Eq.(15),

$$\vec{A}_\mu^{\prime N} \cdot \vec{T} = N \left(\sum_{c=1}^3 A_\mu^c T^c \right) N^\dagger + \text{thin vortex}, \quad (31)$$

where the first term on the right-hand side is regular and the second term indicates a topological defect. Replacing Eqs.(27) and (29) in Eq.(31), one obtains

$$\vec{A}_\mu^{\prime N} \cdot \vec{T} = [A_\mu^1 \cos \varphi + A_\mu^2 \sin \varphi] T^1 \\ + [-A_\mu^1 \sin \varphi + A_\mu^2 \cos \varphi] T^2 \\ + \left[A_\mu^3 - \frac{1}{g} \partial_\mu \varphi \right] T^3 \quad (32)$$

The magnetic vortex flux Φ^{flux} is

$$\Phi^{\text{flux}} = \int dx^\mu (\vec{V}_\mu \cdot \vec{T}) = -\frac{1}{2g} \int_0^{2\pi} d\varphi \begin{pmatrix} 1 & 0 \\ 0 & -1 \end{pmatrix} \\ = -\frac{2\pi}{g} T^3. \quad (33)$$

The total contribution of the magnetic flux is in the third direction in color space.

Using Eq.(25) of Sec. IIIB for the transformed field strength,

$$\vec{F}_{\mu\nu}^{\prime N} \cdot \vec{T} = \left(\partial_\mu (\vec{A}_\nu^{\prime N} \cdot \vec{T}) - \partial_\nu (\vec{A}_\mu^{\prime N} \cdot \vec{T}) \right) + ig \left[\vec{A}_\mu^{\prime N} \cdot \vec{T}, \vec{A}_\nu^{\prime N} \cdot \vec{T} \right] + \frac{i}{g} N [\partial_\mu, \partial_\nu] N^\dagger. \quad (34)$$

With the help of Eq.(32), we rewrite the first term of Eq.(34) which is linear in terms of $\vec{A}'_{\mu}{}^N \cdot \vec{T}$,

$$\begin{aligned}
F_{\mu\nu}^{\text{linear}} &= \vec{F}_{\mu\nu}^{\text{linear}} \cdot \vec{T} \equiv \partial_{\mu} \left(\vec{A}'_{\nu}{}^N \cdot \vec{T} \right) - \partial_{\nu} \left(\vec{A}'_{\mu}{}^N \cdot \vec{T} \right) \\
&= [(\partial_{\mu} A_{\nu}^1 - \partial_{\nu} A_{\mu}^1) \cos\varphi + (\partial_{\mu} A_{\nu}^2 - \partial_{\nu} A_{\mu}^2) \sin\varphi] T^1 + [-(\partial_{\mu} A_{\nu}^1 - \partial_{\nu} A_{\mu}^1) \sin\varphi + (\partial_{\mu} A_{\nu}^2 - \partial_{\nu} A_{\mu}^2) \cos\varphi] T^2 \\
&+ [\partial_{\mu} A_{\nu}^3 - \partial_{\nu} A_{\mu}^3] T^3 + \left[-g \left(A_{\nu}^1 \frac{1}{g} \partial_{\mu} \varphi - A_{\mu}^1 \frac{1}{g} \partial_{\nu} \varphi \right) \sin\varphi + g \left(A_{\nu}^2 \frac{1}{g} \partial_{\mu} \varphi - A_{\mu}^2 \frac{1}{g} \partial_{\nu} \varphi \right) \cos\varphi \right] T^1 \\
&+ \left[-g \left(A_{\nu}^1 \frac{1}{g} \partial_{\mu} \varphi - A_{\mu}^1 \frac{1}{g} \partial_{\nu} \varphi \right) \cos\varphi - g \left(A_{\nu}^2 \frac{1}{g} \partial_{\mu} \varphi - A_{\mu}^2 \frac{1}{g} \partial_{\nu} \varphi \right) \sin\varphi \right] T^2 + \left(-\frac{1}{g} [\partial_{\mu}, \partial_{\nu}] \varphi \right) T^3.
\end{aligned} \tag{35}$$

The first three sets of brackets of Eq.(35) are regular, and the fourth and the fifth sets of brackets indicate some kind of interactions between thin vortex and the off-diagonal gluon fields. $\left(-\frac{1}{g} [\partial_{\mu}, \partial_{\nu}] \varphi \right) T^3$ represents

the field strength of a thin vortex field carrying a magnetic flux, which is equal to $\Phi^{\text{flux}} = -\frac{2\pi}{g} T^3$. The second term of Eq.(34) can be written with the help of Eq.(32),

$$\begin{aligned}
F_{\mu\nu}^{\text{bilinear}} &= \vec{F}_{\mu\nu}^{\text{bilinear}} \cdot \vec{T} \equiv ig \left[\vec{A}'_{\mu}{}^N \cdot \vec{T}, \vec{A}'_{\nu}{}^N \cdot \vec{T} \right] \\
&= [g (A_{\mu}^1 A_{\nu}^3 - A_{\nu}^1 A_{\mu}^3) \sin\varphi - g (A_{\mu}^2 A_{\nu}^3 - A_{\nu}^2 A_{\mu}^3) \cos\varphi] T^1 + [g (A_{\mu}^1 A_{\nu}^3 - A_{\nu}^1 A_{\mu}^3) \cos\varphi + g (A_{\mu}^2 A_{\nu}^3 - A_{\nu}^2 A_{\mu}^3) \sin\varphi] T^2 \\
&+ g [A_{\mu}^2 A_{\nu}^1 - A_{\nu}^2 A_{\mu}^1] T^3 - \left[-g \left(A_{\nu}^1 \frac{1}{g} \partial_{\mu} \varphi - A_{\mu}^1 \frac{1}{g} \partial_{\nu} \varphi \right) \sin\varphi + g \left(A_{\nu}^2 \frac{1}{g} \partial_{\mu} \varphi - A_{\mu}^2 \frac{1}{g} \partial_{\nu} \varphi \right) \cos\varphi \right] T^1 \\
&- \left[-g \left(A_{\nu}^1 \frac{1}{g} \partial_{\mu} \varphi - A_{\mu}^1 \frac{1}{g} \partial_{\nu} \varphi \right) \cos\varphi - g \left(A_{\nu}^2 \frac{1}{g} \partial_{\mu} \varphi - A_{\mu}^2 \frac{1}{g} \partial_{\nu} \varphi \right) \sin\varphi \right] T^2.
\end{aligned} \tag{36}$$

The first three brackets of Eq.(36) represent interactions between gluon fields and are regular. The fourth and the fifth brackets indicate interactions between the thin vortex and off-diagonal gluon fields but with an opposite sign compared with their counterparts in Eq.(35). Back to Eq.(34), the last term can be rewritten with the help of Eq.(27),

$$\vec{F}_{\mu\nu}^{\text{singular}} \cdot \vec{T} \equiv \frac{i}{g} N [\partial_{\mu}, \partial_{\nu}] N^{\dagger} = \frac{1}{g} [\partial_{\mu}, \partial_{\nu}] \varphi T^3. \tag{37}$$

$F_{\mu\nu}^{\text{singular}} = \vec{F}_{\mu\nu}^{\text{singular}} \cdot \vec{T}$ in the above equation indicates the field strength of an anti-thin vortex carrying a magnetic flux equal to $\Phi^{\text{flux}} = +\frac{2\pi}{g} T^3$.

$$\begin{aligned}
\vec{F}_{\mu\nu}^{\text{CP}} \cdot \vec{T} &\equiv \vec{F}_{\mu\nu}^{\text{linear}} \cdot \vec{T} + \vec{F}_{\mu\nu}^{\text{bilinear}} \cdot \vec{T} \\
&= [(\partial_{\mu} A_{\nu}^1 - \partial_{\nu} A_{\mu}^1) \cos\varphi + (\partial_{\mu} A_{\nu}^2 - \partial_{\nu} A_{\mu}^2) \sin\varphi + g (A_{\mu}^1 A_{\nu}^3 - A_{\nu}^1 A_{\mu}^3) \sin\varphi - g (A_{\mu}^2 A_{\nu}^3 - A_{\nu}^2 A_{\mu}^3) \cos\varphi] T^1 \\
&+ [-(\partial_{\mu} A_{\nu}^1 - \partial_{\nu} A_{\mu}^1) \sin\varphi + (\partial_{\mu} A_{\nu}^2 - \partial_{\nu} A_{\mu}^2) \cos\varphi + g (A_{\mu}^1 A_{\nu}^3 - A_{\nu}^1 A_{\mu}^3) \cos\varphi + g (A_{\mu}^2 A_{\nu}^3 - A_{\nu}^2 A_{\mu}^3) \sin\varphi] T^2 \\
&+ [\partial_{\mu} A_{\nu}^3 - \partial_{\nu} A_{\mu}^3 + g (A_{\mu}^2 A_{\nu}^1 - A_{\nu}^2 A_{\mu}^1)] T^3 + \left(-\frac{1}{g} [\partial_{\mu}, \partial_{\nu}] \varphi \right) T^3.
\end{aligned} \tag{38}$$

All the terms in Eq.(38) are regular except the last term,

which represents the field strength of a thin vortex field.

Therefore, the gauge symmetry is $SO(3)$, and thin vortices appear as the topological defects corresponding to the non-trivial first homotopy group $\Pi_1(SO(3)) = Z_2$.

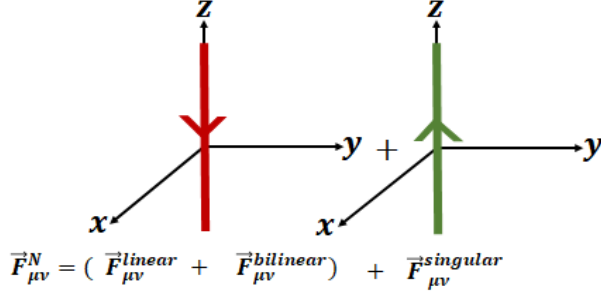


FIG. 2: Appearance of a vortex and an anti-vortex under center gauge transformation.

V. INDIRECT METHOD OF INTRODUCING VORTICES IN THE CONTINUUM

In this section, motivated by the IMCG method in lattice QCD which confirms the existence of vortices,

$$U_\mu^{NM} = 1 + iag \left(N(x) \left[M(x) A_\mu M^\dagger(x) - \frac{i}{g} M(x) \partial_\mu M^\dagger(x) \right] N^\dagger(x) - \frac{i}{g} N(x) \partial_\mu N^\dagger(x) \right) + \mathcal{O}(a^2) \\ = e^{iag A_\mu^{NM}}.$$

$N(x)$ indicates a center gauge transformation, and the contribution of vortices must be obtained from this gauge

$$\vec{A}_\mu^{NM} \cdot \vec{T} = N(x) \left[M(x) (A_\mu^c T^c) M^\dagger(x) - \frac{i}{g} M(x) \partial_\mu M^\dagger(x) \right] N^\dagger(x) + \text{thin vortex}.$$

This is somehow similar to an Abelian gauge fixing plus center gauge fixing of IMCG method in lattice calculations. However, an intermediate step including Abelian projection must be applied, and we discuss it for the $SU(2)$ gauge group in Sec. VI.

we study vortices in the continuum. As mentioned in Sec. II B, in the indirect method, in addition to the center gauge transformation and center projection [19], an initial step including Abelian gauge transformation and then Abelian projection is done.

Two successive gauge transformations are performed such that the first one is an Abelian gauge transformation $M(x) \in SU(N)$ and the second one is a center gauge transformation $N(x) \in SU(N)$. The transformation of link variables is

$$U_\mu(x) \xrightarrow{M(x)} U_\mu^M(x) \xrightarrow{N(x)} U_\mu^{NM}(x) \quad (39)$$

or

$$U_\mu^{NM}(x) = N(x) U_\mu^M(x) N^\dagger(x + \hat{\mu}) \\ = N(x) M(x) U_\mu(x) M^\dagger(x + \hat{\mu}) N^\dagger(x + \hat{\mu}) \\ = N(x) M(x) e^{iag A_\mu} M^\dagger(x + \hat{\mu}) N^\dagger(x + \hat{\mu}). \quad (40)$$

In the last equality, we used Eq.(4). Similar to what we have done in Sec. III A, we can use the exponential expansion and by using the Taylor expansion for $M^\dagger(x + \hat{\mu})$ and $N^\dagger(x + \hat{\mu})$,

For the continuum limit where $a \rightarrow 0$,

transformation. Therefore, similar to the Sec. III A and Eq.(15), the gauge field in the coset space is written as

VI. INDIRECT METHOD OF INTRODUCING VORTICES IN $SU(2)$ GAUGE GROUP

In this section, we apply the procedure explained in the previous section to the $SU(2)$ gauge group, and we

show that, unlike Sec. IV where we have gotten vortices as a result of center gauge transformation and a “center projection”, we get a chain of vortices and monopole by the indirect method.

We discuss this section in two subsections. In Sec. VIA, we study the Abelian gauge transformation and Abelian projection, which leads to the emergence of the monopole.

In Sec. VIB, in addition to steps 1° and 2 in Sec. VIA, a center gauge transformation followed by a “center projection” which leads to the appearance of chains containing vortices and monopoles, is discussed.

A. Abelian gauge tTransformations and Abelian projection: Monopole

The appearance of monopoles relies upon Abelian gauge transformation followed by an Abelian projection, which is discussed in this subsection for the SU(2) gauge group.

Lattice studies show that within a good approximation the string tension between a pair of quark and anti-quark is described by Abelian variables of the maximal Abelian gauge transformation. Therefore, in the continuum limit, the idea of the Abelian gauge transformation is to repress the contribution of the off-diagonal components of the gauge fields so that the contribution of diagonal compo-

nents is dominant in the low-energy regime.

We perform a local rotation in color space called an Abelian gauge transformation. As a result, magnetic monopoles can be extracted from the diagonal part of the non-Abelian gauge field.

Step 1: Abelian gauge transformation Choosing $\alpha(x) = \varphi$, $\beta(x) = \theta$ and $\gamma(x) = \pm\varphi$ in the gauge rotation matrix of Eq.(26), an appropriate gauge transformation $M(x) \in \text{SU}(2)$ which leads to an Abelian gauge transformation, is obtained.

In this paper, we choose $\gamma(x) = -\varphi$,

$$M(\theta, \varphi) = \begin{pmatrix} \cos\frac{\theta}{2} & e^{-i\varphi}\sin\frac{\theta}{2} \\ -e^{i\varphi}\sin\frac{\theta}{2} & \cos\frac{\theta}{2} \end{pmatrix}. \quad (44)$$

According to Sec. IIIA, we define $G(x) \equiv M(x)$ as an Abelian gauge transformation; then the transformation of gluon field is given by Eq.(9),

$$\vec{A}_\mu^M \cdot \vec{T} = M(x) \left(\sum_{c=1}^3 A_\mu^c T^c \right) M^\dagger(x) - \frac{i}{g} M(x) \partial_\mu M^\dagger(x). \quad (45)$$

The first term on the right-hand side of Eq.(45) is regular under Abelian gauge transformation $M(x)$, but the second term is singular. Replacing Eq.(44) in Eq.(45),

$$\begin{aligned} \vec{A}_\mu^M \cdot \vec{T} = & \left[A_\mu^1 \left(1 - 2\sin^2\frac{\theta}{2}\cos^2\varphi \right) + A_\mu^2 \left(-\sin^2\frac{\theta}{2}\sin 2\varphi \right) + A_\mu^3 (-\sin\theta\cos\varphi) + \frac{1}{g}\sin\varphi\partial_\mu\theta + \frac{1}{g}\sin\theta\cos\varphi\partial_\mu\varphi \right] T^1 \\ & + \left[A_\mu^1 \left(-\sin^2\frac{\theta}{2}\sin 2\varphi \right) + A_\mu^2 \left(1 - 2\sin^2\frac{\theta}{2}\sin^2\varphi \right) + A_\mu^3 (-\sin\theta\sin\varphi) - \frac{1}{g}\cos\varphi\partial_\mu\theta + \frac{1}{g}\sin\theta\sin\varphi\partial_\mu\varphi \right] T^2 \\ & + \left[A_\mu^1 (\sin\theta\cos\varphi) + A_\mu^2 (\sin\theta\sin\varphi) + A_\mu^3 (\cos\theta) + \frac{1}{g}(1 - \cos\theta)\partial_\mu\varphi \right] T^3, \end{aligned} \quad (46)$$

where the singularity appears in the inhomogeneous term of the above equation defined by $A_\mu^{\text{singular}}(\theta, \varphi) =$

$A_\mu^{\text{singular}}(\theta, \varphi)T^c \equiv -\frac{i}{g}M(\theta, \varphi)\partial_\mu M^\dagger(\theta, \varphi)$ in spherical coordinates and is given by

$$\begin{aligned} \mathbf{A}^{\text{singular}}(\theta, \varphi) = & -\frac{i}{g}M(\theta, \varphi)\nabla M^\dagger(\theta, \varphi) = \frac{1}{2g} \begin{pmatrix} [1 - \cos\theta]\nabla\varphi & [i\nabla\theta + \sin\theta\nabla\varphi]e^{-i\varphi} \\ [-i\nabla\theta + \sin\theta\nabla\varphi]e^{i\varphi} & -[1 - \cos\theta]\nabla\varphi \end{pmatrix} \\ & = \frac{g^{-1}}{r}(\cos\varphi\mathbf{e}_\varphi + \sin\varphi\mathbf{e}_\theta)T^1 + \frac{g^{-1}}{r}(\sin\varphi\mathbf{e}_\varphi - \cos\varphi\mathbf{e}_\theta)T^2 + \frac{g^{-1}}{r}\frac{1 - \cos\theta}{\sin\theta}\mathbf{e}_\varphi T^3, \end{aligned} \quad (47)$$

where $\mathbf{A}^{\text{singular}}(\theta, \varphi) = \mathbf{A}^{\text{c singular}}(\theta, \varphi)T^c$. It is observed from Eq.(47) that there exists a magnetic monopole as a point defect at the origin, $r = 0$ along with a Dirac string

at $\theta = \pi$.

The magnetic flux $\Phi^{\text{flux}}(\theta)$ of the inhomogeneous term is given by

$$\begin{aligned}\Phi^{\text{flux}}(\theta) &= \int_c dx^\mu A_\mu^{\text{singular}}(\theta, \varphi) = \frac{1}{2g} \int_0^{2\pi} d\varphi \begin{pmatrix} 1 - \cos\theta & \sin\theta e^{-i\varphi} \\ \sin\theta e^{i\varphi} & -(1 - \cos\theta) \end{pmatrix} \\ &= \frac{2\pi}{2g} \begin{pmatrix} 1 - \cos\theta & 0 \\ 0 & -(1 - \cos\theta) \end{pmatrix} = \frac{2\pi}{g} (1 - \cos\theta) T^3.\end{aligned}\quad (48)$$

It is observed that the total contribution of the magnetic flux is located along the third direction of the color space. At $\theta = \pi$, the magnetic flux of a Dirac string that enters a monopole located at the origin $r = 0$ is equal to $\frac{4\pi}{g} T^3$.

We have discussed in Sec. III B that under a gauge transformation, the field strength tensor is obtained from Eq.(25). We rewrite it as follows:

$$\begin{aligned}\vec{F}_{\mu\nu}^M \cdot \vec{T} &= \left(\partial_\mu \left(\vec{A}_\nu^M \cdot \vec{T} \right) - \partial_\nu \left(\vec{A}_\mu^M \cdot \vec{T} \right) \right) \\ &+ ig \left[\vec{A}_\nu^M \cdot \vec{T}, \vec{A}_\mu^M \cdot \vec{T} \right] \\ &+ \frac{i}{g} M(\theta, \varphi) [\partial_\mu, \partial_\nu] M^\dagger(\theta, \varphi).\end{aligned}\quad (49)$$

Equation (49) can be calculated using Eqs.(44) and (46). Since the two color directions T^1 and T^2 have no contribution in the magnetic flux, we will suppress these non-diagonal components of the gauge fields in the ‘‘Abelian projection’’ step. It can be easily confirmed that the first term of the Abelian sector $(F_{\mu\nu}^{\text{linear}})^3 \equiv \partial_\mu (A_\nu^M)^3 - \partial_\nu (A_\mu^M)^3$ includes a magnetic monopole sitting at the origin along with a Dirac string in $\theta = \pi$. The second term of the Abelian sector is called $(F_{\mu\nu}^{\text{bilinear}})^3 \equiv -g \left\{ (A_\mu^M)^1 (A_\nu^M)^2 - (A_\mu^M)^2 (A_\nu^M)^1 \right\}$ and contains an anti-monopole at the origin, and the third term of the Abelian sector $F_{\mu\nu}^{\text{singular}} \equiv \frac{i}{g} M(\theta, \varphi) [\partial_\mu, \partial_\nu] M^\dagger(\theta, \varphi)$ includes an anti-Dirac string at $\theta = \pi$ with a magnetic flux equal to $-\frac{4\pi}{g} T^3$. (See Appendix A and Fig.(3)),

$$F_{\mu\nu}^M = F_{\mu\nu}^{\text{linear}} + F_{\mu\nu}^{\text{singular}} + F_{\mu\nu}^{\text{bilinear}}.\quad (50)$$

As a result, $F_{\mu\nu}^{\text{bilinear}}$, which gives the anti-monopole contribution, is equal to zero, and the remaining part $F_{\mu\nu}^{\text{linear}} + F_{\mu\nu}^{\text{singular}}$ describes an Abelian projected QCD, which contains a monopole at $r = 0$ and is called the monopole vacuum.

After Abelian projection, SU(2) gauge symmetry is reduced to U(1) gauge symmetry, and monopoles appear as the topological defects corresponding to the non-trivial

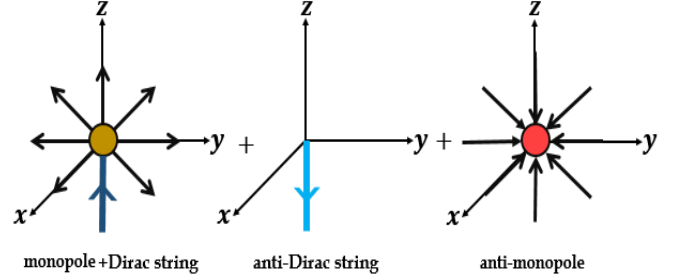


FIG. 3: Appearance of a monopole accompanying a Dirac-string, an anti-Dirac string, and an anti-monopole as a result of an Abelian gauge transformation.

If we add the contents of the above three terms, the similar terms with opposite signs are canceled, and a field strength tensor which gives a full QCD is obtained [12].

Step 2: Abelian projection The sum of the two terms $F_{\mu\nu}^{\text{linear}} + F_{\mu\nu}^{\text{singular}}$ represents a gauge configuration that only contains a monopole at $r = 0$. However, it is exactly canceled by the anti-monopole arisen from $F_{\mu\nu}^{\text{bilinear}}$. Thus, one can claim that the vacuum is filled with monopoles and anti-monopoles.

From Fig.(3), it is observed that, in order to have only the contribution of the monopole, we discard the term $F_{\mu\nu}^{\text{bilinear}}$ so that [12]

$$\vec{A}_\mu^M \cdot \vec{T} = (A_\mu^M)^a T^a \rightarrow \mathcal{A}_\mu \equiv (A_\mu^M)^3 T^3.\quad (51)$$

From Eq.(46), the gauge field is changed to

$$\mathcal{A}_\mu = \left[A_\mu^1 (\sin\theta \cos\varphi) + A_\mu^2 (\sin\theta \sin\varphi) + A_\mu^3 (\cos\theta) + \frac{1}{g} (1 - \cos\theta) \partial_\mu \varphi \right] T^3.\quad (52)$$

second homotopy group $\Pi_2(\text{SU}(2)/\text{U}(1)) = \mathbb{Z}$.

B. Center gauge transformation and ‘‘Center Projection’’: Chain

As mentioned before, the vortex recognition by the indirect method is done in four steps. We have discussed the first two steps in Sec. VIA and we explain the final

two steps in the following.

Step 3: Center gauge transformation; We have shown that under two successive gauge transformations the gluon field is changed by Eq.(43). After Abelian projection, the bracket in Eq.(43) should be replaced by

$$\begin{aligned} \vec{A}'_{\mu}{}^{NM} \cdot \vec{T} &= \left[A_{\mu}^1 (\sin\theta \cos\varphi) + A_{\mu}^2 (\sin\theta \sin\varphi) + A_{\mu}^3 (\cos\theta) + \frac{1}{g} (1 - \cos\theta) \partial_{\mu}\varphi - \frac{1}{g} \partial_{\mu}\varphi \right] T^3 \\ &= \left[A_{\mu}^1 (\sin\theta \cos\varphi) + A_{\mu}^2 (\sin\theta \sin\varphi) + A_{\mu}^3 (\cos\theta) - \frac{1}{g} \cos\theta \partial_{\mu}\varphi \right] T^3. \end{aligned} \quad (54)$$

The first three terms on the right-hand side of Eq.(54) are regular, and the last term is defined in the spherical coordinates as $\left(-\frac{1}{g} \cos\theta \partial_{\mu}\varphi T^3 = -\frac{g^{-1} \cos\theta}{r \sin\theta} \mathbf{e}_{\varphi} T^3 \right)$. It indicates a defect representing a monopole located at the origin $r = 0$ along with the two vortices at $\theta = 0, \pi$. This singular term remarkably represents a chain containing monopole and vortices. In fact, the magnetic potential

Eq.(51),

$$\vec{A}'_{\mu}{}^{NM} \cdot \vec{T} = N(x) \mathcal{A}_{\mu} N^{\dagger}(x) + \text{thin vortex}. \quad (53)$$

For $x \notin$ hypersurface, the thin vortex is defined in Eq.(16).

In fact, Eq.(53) expresses that a center gauge transformation is applied on a monopole vacuum. Using the center gauge transformation defined by Eq.(27) and the Abelian projected field defined by Eq.(52), the above equation is changed to

of the chain defined by $E_{\mu} \equiv -\frac{1}{g} \cos\theta \partial_{\mu}\varphi T^3$, can be interpreted as the sum of two terms: a magnetic potential of a monopole along with a Dirac string defined by $B_{\mu} \equiv \frac{1}{g} (1 - \cos\theta) \partial_{\mu}\varphi T^3$ plus a magnetic potential of a vortex defined by $V_{\mu} \equiv -\frac{1}{g} \partial_{\mu}\varphi T^3$.

The magnetic flux $\Phi^{\text{flux}}(\theta)$ passing through a closed contour $C(r, \theta)$ is defined as

$$\begin{aligned} \Phi^{\text{flux}}(\theta) &= \int_c dx^{\mu} A'_{\mu}{}^{\text{singular}} = \frac{2\pi}{2g} \begin{pmatrix} 1 - \cos\theta & 0 \\ 0 & -(1 - \cos\theta) \end{pmatrix} - \frac{2\pi}{2g} \begin{pmatrix} 1 & 0 \\ 0 & -1 \end{pmatrix} \\ &= \frac{2\pi}{g} (1 - \cos\theta) T^3 - \frac{2\pi}{g} T^3 \\ &= -\frac{2\pi}{g} \cos\theta T^3, \end{aligned} \quad (55)$$

where the first term in the second line of Eq.(55) represents the magnetic monopole flux plus a Dirac string. At $\theta = \pi$, the contribution of the flux of the Dirac string is equal to $+\frac{4\pi}{g} T^3$. The second term in the second line of Eq.(55) indicates a vortex extending on the z axis with a flux equal to $-\frac{2\pi}{g} T^3$. Finally, the chain flux is obtained as the sum of the vortex flux and the magnetic monopole flux plus the Dirac string and is equal to $-\frac{2\pi}{g} \cos\theta T^3$.

Now, we have some discussions about the chain characteristic. From Eq.(55) for $\theta = 0$, we only have the contribution of a magnetic vortex flux equal to $-\frac{2\pi}{g} T^3$, located in the positive direction of the z axis which enters

the magnetic monopole placed at the origin, $r = 0$. At $\theta = \pi$, there exists a Dirac string flux equal to $+\frac{4\pi}{g} T^3$ located in the negative direction of the z axis and entering the magnetic monopole. There is also a magnetic vortex whose flux is equal to $-\frac{2\pi}{g} T^3$ at $\theta = \pi$. It is located in the negative direction of the z axis and exits from the magnetic monopole placed at $r = 0$. In fact, the sum of the two fluxes $\Phi^{\text{Dirac string}} + \Phi^{\text{line vortex}}$ represents the contribution of a vortex equal to $+\frac{2\pi}{g} T^3$, which enters the magnetic monopole sitting at the origin, $r = 0$. As a result, the magnetic flux of the monopole is obtained as the sum of the absolute values of the fluxes of the two vortices entering into it.

Equation (25) is used to obtain the field strength tensor of the transformation,

$$\begin{aligned}
\vec{F}_{\mu\nu}^{NM} \cdot \vec{T} &= N(x) \left(\vec{F}_{\mu\nu}^M \cdot \vec{T} \right) N^\dagger(x) = N(x) M(x) \left(\vec{F}_{\mu\nu} \cdot \vec{T} \right) M^\dagger(x) N^\dagger(x) \\
&= \frac{1}{ig} \left[\hat{D}_\mu^{NM}, \hat{D}_\nu^{NM} \right] - \frac{1}{ig} N(x) M(x) \left[\hat{\partial}_\mu, \hat{\partial}_\nu \right] M^\dagger(x) N^\dagger(x) \\
&= \left(\partial_\mu \left(\vec{A}_\nu^{NM} \cdot \vec{T} \right) - \partial_\nu \left(\vec{A}_\mu^{NM} \cdot \vec{T} \right) \right) + ig \left[\vec{A}_\mu^{NM} \cdot \vec{T}, \vec{A}_\nu^{NM} \cdot \vec{T} \right] + \frac{i}{g} N(x) M(x) [\partial_\mu, \partial_\nu] M^\dagger(x) N^\dagger(x).
\end{aligned} \tag{56}$$

We use Eq.(56) to study some various topological defects. A full QCD is obtained if one uses Eq.(56) without applying any projection. In this section, we discuss the possible resulting defects after Abelian and ‘‘center projections’’.

Looking at the last line of Eq.(56), we define the first term by $F_{\mu\nu}^{\text{linear}} = \vec{F}_{\mu\nu}^{\text{linear}} \cdot \vec{T} \equiv \partial_\mu \left(\vec{A}_\nu^{NM} \cdot \vec{T} \right) - \partial_\nu \left(\vec{A}_\mu^{NM} \cdot \vec{T} \right)$ and rewrite it using Eq.(54),

$$\begin{aligned}
\vec{F}_{\mu\nu}^{\text{linear}} \cdot \vec{T} &= \left\{ (\partial_\mu A_\nu^1 - \partial_\nu A_\mu^1) \sin\theta \cos\varphi + A_\nu^1 \partial_\mu (\sin\theta \cos\varphi) - A_\mu^1 \partial_\nu (\sin\theta \cos\varphi) \right\} T^3 \\
&\quad + \left\{ (\partial_\mu A_\nu^2 - \partial_\nu A_\mu^2) \sin\theta \sin\varphi + A_\nu^2 \partial_\mu (\sin\theta \sin\varphi) - A_\mu^2 \partial_\nu (\sin\theta \sin\varphi) \right\} T^3 \\
&\quad + \left\{ (\partial_\mu A_\nu^3 - \partial_\nu A_\mu^3) \cos\theta + A_\nu^3 \partial_\mu (\cos\theta) - A_\mu^3 \partial_\nu (\cos\theta) \right\} T^3 \\
&\quad + (\partial_\mu E_\nu - \partial_\nu E_\mu) T^3.
\end{aligned} \tag{57}$$

The last line of the above equation contains some defects as explained in the following:

$$\begin{aligned}
(\partial_\mu E_\nu - \partial_\nu E_\mu) T^3 &= \frac{1}{g} \sin\theta (\partial_\mu \theta \partial_\nu \varphi - \partial_\mu \varphi \partial_\nu \theta) T^3 \\
&\quad + \frac{1}{g} (1 - \cos\theta) [\partial_\mu, \partial_\nu] \varphi T^3 \\
&\quad - \frac{1}{g} [\partial_\mu, \partial_\nu] \varphi T^3.
\end{aligned} \tag{58}$$

The first term of Eq.(58) represents the field strength of a magnetic monopole located at $r = 0$, the second term indicates the field strength of a Dirac string at $\theta = \pi$, and the third term represents the field strength of a thin vortex field that extended on the z axis. (See Fig.(4).)

It is clear that the second term of Eq.(56), $\vec{F}_{\mu\nu}^{\text{bilinear}} \cdot \vec{T} \equiv ig \left[\vec{A}_\mu^{NM}(x) \cdot \vec{T}, \vec{A}_\nu^{NM}(x) \cdot \vec{T} \right]$, is zero. This happens because of the Abelian projection process which makes the components of the gluon field zero for the two color directions T^1 and T^2 . Using the center gauge transformation defined in Eq.(27) and the Abelian gauge transformation

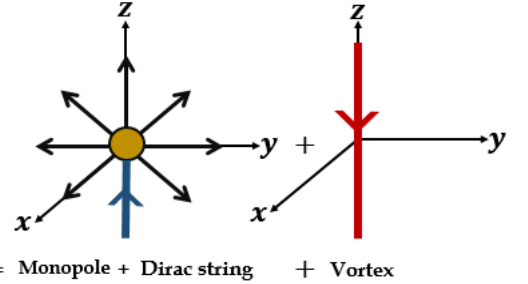


FIG. 4: Appearance of a monopole attached to a Dirac-string and a vortex after Abelian gauge transformation, Abelian projection, and center gauge transformation.

of Eq.(44), the third term of Eq.(56) is

$$\begin{aligned}
F_{\mu\nu}^{\text{singular}} &= \vec{F}_{\mu\nu}^{\text{singular}} \cdot \vec{T} \\
&= -\frac{1}{g} (1 - \cos\theta) [\partial_\mu, \partial_\nu] \varphi T^3 + \frac{1}{g} [\partial_\mu, \partial_\nu] \varphi T^3 \\
&= \frac{1}{g} \cos\theta [\partial_\mu, \partial_\nu] \varphi T^3,
\end{aligned} \tag{59}$$

where $-\frac{1}{g} (1 - \cos\theta) [\partial_\mu, \partial_\nu] \varphi T^3$ represents the field strength of an anti-Dirac string in $\theta = \pi$ with a flux

equal to $-\frac{4\pi}{g}T^3$ and the term $\frac{1}{g}[\partial_\mu, \partial_\nu]\varphi T^3$ represents the field strength of an anti-vortex on the z axis with a flux equal to $+\frac{2\pi}{g}T^3$. (See Fig.(5))

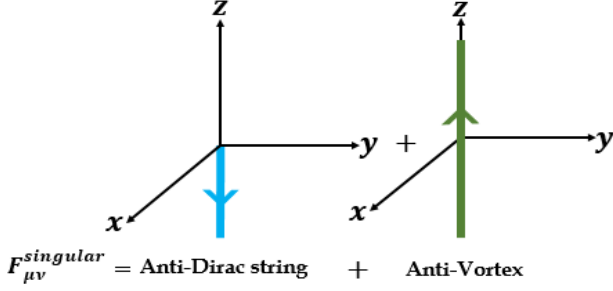


FIG. 5: Appearance of an anti-Dirac string and an anti-vortex after Abelian gauge transformation, followed by an Abelian projection and then a center gauge transformation.

In fact, the contribution of the vortex and the Dirac string appearing in $F_{\mu\nu}^{\text{linear}}$ is exactly canceled by the contribution of the anti-vortex and the anti-Dirac string in $F_{\mu\nu}^{\text{singular}}$. As a result, a monopole vacuum is obtained unless we remove some of the singularities from the theory.

Step 4: “Center projection” As explained in Sec. IV, a “center projection” is done by removing $F_{\mu\nu}^{\text{singular}}$ defined in Eq.(59). This means that “center projection” is obtained by $F_{\mu\nu}^{\text{linear}} + F_{\mu\nu}^{\text{bilinear}}$. On the other hand, we have shown that $F_{\mu\nu}^{\text{bilinear}}$ is zero, and as a result, the center projected field strength tensor is as follows:

$$F_{\mu\nu}^{\text{CP}} = F_{\mu\nu}^{\text{linear}}. \quad (60)$$

Therefore, only a monopole attached to a Dirac string and a vortex remain. We can interpret these configuration as a chain as shown in Fig.(6).

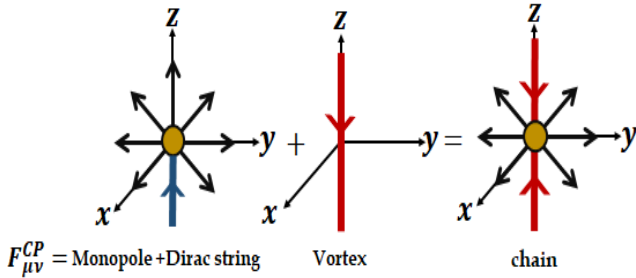


FIG. 6: Appearance of a chain after Abelian gauge transformation, Abelian projection, center gauge transformation, and “center projection”.

The first plot on the left-hand side of Fig.(6) represents a monopole at $r = 0$ plus a Dirac string located

at $\theta = \pi$ carrying a magnetic flux equal to $\frac{4\pi}{g}T^3$. The second plot on the left-hand side indicates a vortex carrying a magnetic flux equal to $-\frac{2\pi}{g}T^3$ extending on the z axis. Combining these two plots, a chain shown on the right-hand side of Fig.(6) is obtained. A chain contains a monopole at $r = 0$ and two vortices entering it. The flux of the vortex sitting at $\theta = 0$ is equal to $-\frac{2\pi}{g}T^3$, and the flux of the vortex sitting at $\theta = \pi$ is equal to $+\frac{2\pi}{g}T^3$. The latter vortex is obtained as a result of combining the flux of the Dirac string sitting in the negative z direction and the first vortex located in the z direction.

Our arguments about the chains of monopoles and vortices are in agreement with the work of Del Debbio *et al.* [24], which is done by lattice QCD (see Fig.(7)), and also in agreement with the results of Reinhardt and Engelhardt [41], in which two vortex enter a monopole (see Fig.(8)).

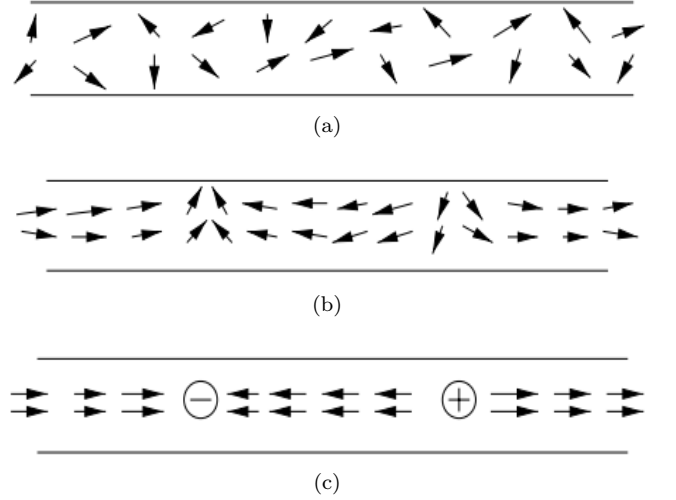


FIG. 7: Vortex field strength: (a) before gauge fixing, (b) after maximal Abelian gauge fixing in the horizontal $\pm\sigma^3$ direction, and (c) after Abelian projection [24]. As shown in this figure, two vortex lines enter a monopole or an anti-monopole, in agreement with what we have introduced in this paper as a chain configuration in Fig. (6).

We end this section by discussing the possible advantages of using chains. As we mentioned at the beginning of the article, in both the dual superconductor model and the center vortex model, monopoles and vortices can explain some aspects of the color confinement like the linear potential between a quark and anti-quark. However, none of these models nor the associated defects is able to describe all the expected features of the confining potential between color sources.

At intermediate distances, a well-defined linear con-

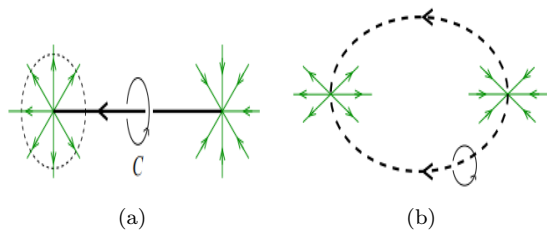


FIG. 8: Illustration of the connection between Dirac string shown in plot (a) and the center vortex shown in plot (b) [41]. The interpretation of a chain represented in Fig. (6) is the same as this figure where two vortex lines enter a monopole.

fining potential is expected, $V_R(r) \sim \sigma_R r$, in which σ_R is the string tension of representation R . The confining potential should agree with the Casimir scaling at intermediate distances. It means that the string tension of the potential between a quark and an anti-quark in representation R , σ_R , is approximately proportional to the quadratic Casimir operator C_R of representation R , i.e.,

$$\sigma_R = \frac{C_R}{C_F} \sigma_F, \quad (61)$$

where F indicates the fundamental representation and σ_F shows the string tension of the fundamental representation. C_F denotes the eigenvalue of the Casimir operator of representation F . We recall that the dependence of the potential slope to the Casimir scaling applies only for the intermediate distances and it is valid and exact for the large N limit [42, 43]. In addition, at large distances, the k -string tension depends on the N -ality of the representation; it is equal to the fundamental representation string tension for the non-zero N -ality representations and zero for the zero N -ality representations [44].

Proportionality with Casimir scaling for the intermediate distances and the N -ality dependence of the potentials at large distances are confirmed by lattice calculations for the fundamental and a variety of higher representations [45–47]. Therefore, any phenomenological model which tries to describe the potential between static color sources is expected to interpret these two features. Vortex based models have been able to explain the N -ality dependence. However, to get the Casimir scaling for all representations, the models have been modified by defining a thickness for the vortex [24, 48]. On the other hand, lattice results confirm the existence of chains of monopoles and vortices [25, 49] that may explain the agreement of the potentials with Casimir scaling for higher representations. In this article, we have followed this approach to study the existence of chains of monopoles and vortices for the continuum.

We recall that an Abelian-projected theory gives the N -ality dependence (after all, it can still contain vortices), but it does not give the Casimir scaling dependence at intermediate distances [23, 50]

In this paper, motivated by direct and indirect methods of identifying vortices in lattice QCD, we have shown the existence of chains of monopoles and vortices for the continuum.

VII. CONCLUSIONS

Motivated by lattice QCD, which discusses the vortex contribution in color confinement, we have tried to introduce vortices in the continuum.

In the absence of matter fields, we work in the quenched approximation where dynamical quarks are removed from the theory. Therefore, the theory includes only the gluon fields, in this limit.

In recent years, the identification of vortices in lattice QCD has seen significant progress. Therefore, one expects to observe the same physics in the continuum limit when one uses the lattice results for the limit where $a \rightarrow 0$.

Inspired by direct and indirect maximal center gauge methods which have studied vortices in lattice calculations and by using connection formalism technique, we have tried to recognize the vortices in the continuum. We have introduced the thin vortices from the gluon fields via both direct and indirect methods for the $SU(N)$ gauge group. We also get some help from the techniques proposed by Engelhardt and Reinhardt.

For an example, from the direct method, we have shown that under center gauge transformation the QCD vacuum of the $SU(2)$ gauge group is filled with the vortices and anti-vortices. Then, applying a “center projection” we reach a theory that contains the thin vortex. The theory has an $SO(3)$ symmetry containing the vortex, which corresponds to the non-trivial first homotopy group of $\Pi_1(SO(3)) = Z_2$.

Then, using the indirect method, we have shown that under Abelian gauge transformation for the $SU(2)$ case the gauge theory would contain monopoles along with the Dirac strings and anti-Dirac strings as well as anti-monopoles. Then, applying Abelian projection and removing the anti-monopole contribution, we end up with a theory that includes only the monopoles. In other words, $SU(2)$ gauge symmetry is reduced to a $U(1)$ gauge symmetry, and monopoles appear as the topological defects corresponding to the non-trivial second homotopy group $\Pi_2(SU(2)/U(1)) = \mathbb{Z}$.

Next, we have done a center gauge transformation on the Abelian vacuum. As a result, we get the monopole along with the Dirac string, the vortex, and anti-Dirac string, and the anti-vortex. Eventually, by applying “center projection”, we end up with a theory that contains chains including monopole and two vortices.

APPENDIX

A. Transformation of field strength tensor under an Abelian gauge transformation

In subsection VI A, we express that the field strength is changed by Eq.(49) when Abelian gauge transformation

is applied. One can also show that,

$$\begin{aligned}\vec{F}_{\mu\nu}^M \cdot \vec{T} &= \vec{F}_{\mu\nu}^{\text{linear}} \cdot \vec{T} + \vec{F}_{\mu\nu}^{\text{bilinear}} \cdot \vec{T} + \vec{F}_{\mu\nu}^{\text{singular}} \cdot \vec{T} \\ &\equiv \left(\partial_\mu \left(\vec{A}_\nu^M \cdot \vec{T} \right) - \partial_\nu \left(\vec{A}_\mu^M \cdot \vec{T} \right) \right) \\ &\quad + ig \left[\vec{A}_\mu^M \cdot \vec{T}, \vec{A}_\nu^M \cdot \vec{T} \right] \\ &\quad + \frac{i}{g} M(\theta, \varphi) [\partial_\mu, \partial_\nu] M^\dagger(\theta, \varphi).\end{aligned}\tag{A.1}$$

Each term of Eq.(A.1) can be expressed in terms of the SU(2) group generators as the following:

$$\begin{aligned}\vec{F}_{\mu\nu}^{\text{linear}} \cdot \vec{T} &= (F_{\mu\nu}^{\text{linear}})^1 T^1 + (F_{\mu\nu}^{\text{linear}})^2 T^2 + (F_{\mu\nu}^{\text{linear}})^3 T^3, \\ \vec{F}_{\mu\nu}^{\text{bilinear}} \cdot \vec{T} &= (F_{\mu\nu}^{\text{bilinear}})^1 T^1 + (F_{\mu\nu}^{\text{bilinear}})^2 T^2 + (F_{\mu\nu}^{\text{bilinear}})^3 T^3, \\ \vec{F}_{\mu\nu}^{\text{singular}} \cdot \vec{T} &= (F_{\mu\nu}^{\text{singular}})^1 T^1 + (F_{\mu\nu}^{\text{singular}})^2 T^2 + (F_{\mu\nu}^{\text{singular}})^3 T^3.\end{aligned}\tag{A.2}$$

From Eq.(46), $\vec{F}_{\mu\nu}^{\text{linear}} \cdot \vec{T}$ is obtained for the Abelian sector

$$\begin{aligned}(F_{\mu\nu}^{\text{linear}})^3 &= (\partial_\mu A_\nu^1 - \partial_\nu A_\mu^1) \sin\theta \cos\varphi + A_\nu^1 \partial_\mu (\sin\theta \cos\varphi) - A_\mu^1 \partial_\nu (\sin\theta \cos\varphi) \\ &\quad + (\partial_\mu A_\nu^2 - \partial_\nu A_\mu^2) \sin\theta \sin\varphi + A_\nu^2 \partial_\mu (\sin\theta \sin\varphi) - A_\mu^2 \partial_\nu (\sin\theta \sin\varphi) \\ &\quad + (\partial_\mu A_\nu^3 - \partial_\nu A_\mu^3) \cos\theta + A_\nu^3 \partial_\mu (\cos\theta) - A_\mu^3 \partial_\nu (\cos\theta) \\ &\quad + \frac{1}{g} \sin\theta (\partial_\mu \theta \partial_\nu \varphi - \partial_\mu \varphi \partial_\nu \theta) + \frac{1}{g} (1 - \cos\theta) [\partial_\mu, \partial_\nu] \varphi,\end{aligned}\tag{A.3}$$

where, $+\frac{1}{g} \sin\theta (\partial_\mu \theta \partial_\nu \varphi - \partial_\mu \varphi \partial_\nu \theta)$ represents the field strength of a magnetic monopole at $r = 0$ and

$\frac{1}{g} (1 - \cos\theta) [\partial_\mu, \partial_\nu] \varphi$ indicates the field strength of a Dirac string at $\theta = \pi$.

The Abelian sector $\vec{F}_{\mu\nu}^{\text{bilinear}} \cdot \vec{T}$ is also obtained by Eq.(46),

$$\begin{aligned}(F_{\mu\nu}^{\text{bilinear}})^3 &= -g (A_\mu^2 A_\nu^3 - A_\mu^3 A_\nu^2) \sin\theta \cos\varphi - A_\nu^1 \partial_\mu (\sin\theta \cos\varphi) + A_\mu^1 \partial_\nu (\sin\theta \cos\varphi) \\ &\quad - g (A_\mu^3 A_\nu^1 - A_\mu^1 A_\nu^3) \sin\theta \sin\varphi - A_\nu^2 \partial_\mu (\sin\theta \sin\varphi) + A_\mu^2 \partial_\nu (\sin\theta \sin\varphi) \\ &\quad - g (A_\mu^1 A_\nu^2 - A_\mu^2 A_\nu^1) \cos\theta - A_\nu^3 \partial_\mu (\cos\theta) + A_\mu^3 \partial_\nu (\cos\theta) \\ &\quad - \frac{1}{g} \sin\theta (\partial_\mu \theta \partial_\nu \varphi - \partial_\mu \varphi \partial_\nu \theta),\end{aligned}\tag{A.4}$$

where $-\frac{1}{g} \sin\theta (\partial_\mu \theta \partial_\nu \varphi - \partial_\mu \varphi \partial_\nu \theta)$ represents the field strength of an anti-monopole at $r = 0$.

by Eq.(44),

$$(F_{\mu\nu}^{\text{singular}})^3 = -\frac{1}{g} (1 - \cos\theta) [\partial_\mu, \partial_\nu] \varphi.\tag{A.5}$$

Finally, $\vec{F}_{\mu\nu}^{\text{singular}} \cdot \vec{T}$ is obtained for the Abelian sector

And the above singular term shows the field strength of an anti-Dirac string at $\theta = \pi$.

-
- [1] R. F. Alvarez-Estrada, F. Fernandez, J. L. Sanchez-Gomez, and V. Vento, *Models of Hadrons Structure Based on Quantum Chromodynamics* (Springer, Berlin, Heidelberg, 1986).
- [2] C. Gatttringer and C. B. Lang, *Quantum Chromodynamics on the Lattice: An Introductory Presentation* (Springer-Verlag, Berlin, Heidelberg, 2010).
- [3] H. Suganuma, N. Ishii, M. Oka, H. Enyo, T. Hatsuda, T. Kunihiro, and K. Yazaki, *International Conference on Color Confinement and Hadrons in Quantum Chromodynamics: The Institute of Physical and Chemical Research* (World Scientific, Singapore, 2004).
- [4] J. Greensite, *An Introduction to the Confinement Problem (Lecture Notes in Physics)* (Springer-Verlag, Berlin, Heidelberg, 2011).
- [5] G. 't Hooft, A property of electric and magnetic flux in non-Abelian gauge theories, *Nucl. Phys.* **B153**, 141 (1979).
- [6] S.V. Shabanov, Yang-Mills theory as an Abelian theory without gauge fixing, *Phys. Lett. B* **463**, 263 (1999).
- [7] L. Faddeev and A.J. Niemi, Decomposing the Yang-Mills field, *Phys. Lett. B* **464**, 90 (1999).
- [8] Y. M. Cho, Restricted gauge theory, *Phys. Rev. D* **21**, 1080 (1980).
- [9] Y. M. Cho, Extended gauge theory and its mass spectrum, *Phys. Rev. D* **23**, 2415 (1981).
- [10] M. Engelhardt, Generation of confinement and other nonperturbative effects by infrared gluonic degrees of freedom, *Nucl. Phys. Proc. Suppl.* **140**, 92 (2005).
- [11] K.-I. Kondo, T. Shinohara, and T. Murakami, Reformulating $SU(N)$ Yang-Mills theory based on change of variables, *Prog. Theor. Phys.* **120**, 1 (2008).
- [12] H. Ichie and H. Suganuma, Dual Higgs theory for color confinement in quantum chromodynamics, arXiv: hep-lat/9906005.
- [13] Y. Nambu, Strings, monopoles, and gauge fields, *Phys. Rev. D* **10**, 4262 (1974).
- [14] S. Mandelstam, Vortices and quark confinement in non-Abelian gauge theories, *Phys. Rep.* **23**, 245 (1976).
- [15] G. 't Hooft, in *High Energy Physics*, edited by A. Zichichi (Editorice Compositori, Bologna, 1975).
- [16] A. Polyakov, Quark confinement and topology of gauge theories, *Nucl. Phys.* **B120**, 429 (1977).
- [17] G. Ripka, Dual superconductor models of color confinement, *Lect. Notes Phys.* 639, 1 (2004).
- [18] K.-I. Kondo, S.Kato, A. Shibata, and T. Shinohara, Quark confinement: Dual superconductor picture based on a non-Abelian Stokes theorem and reformulations of Yang-Mills theory, *Phys. Rep.* **579**, 1 (2015).
- [19] L. D. Debbio, M. Faber, J. Greensite, and S. Olejnik, Center dominance and $Z(2)$ vortices in $SU(2)$ lattice gauge theory, *Phys. Rev. D* **55**, 2298 (1997).
- [20] M. Faber, J. Greensite, and S. Olejnik, Casimir scaling from center vortices: Towards an understanding of the adjoint string tension, *Phys. Rev. D* **57**, 2603 (1998).
- [21] L. D. Debbio, M. Faber, J. Giedt, J. Greensite, and S. Olejnik, Detection of center vortices in the lattice Yang-Mills vacuum, *Phys. Rev. D* **58**, 094501 (1998).
- [22] J. Greensite, The Confinement problem in lattice gauge theory, *Prog. Part. Nucl. Phys.* **51**, 1 (2003).
- [23] L. D. Debbio, M. Faber, J. Greensite, and S. Olejnik, Some cautionary remarks on Abelian projection and Abelian dominance, *Nucl. Phys. Proc. Suppl.* **53**, 141 (1997).
- [24] L. D. Debbio, M. Faber, J. Greensite, and S. Olejnik, Center dominance, center vortices, and confinement, arXiv: hep-lat/9708023.
- [25] J. Ambjorn, J. Giedt, and J. Greensite, Vortex structure versus monopole dominance in Abelian projected gauge theory, *J. High Energy Phys.* **02**, (2000) 033.
- [26] A. A. Abrikosov, Nobel lecture: Type-II superconductors and the vortex lattice, *Rev. Mod. Phys.* **76**, 975 (2004).
- [27] G. 't Hooft, On the phase transition towards permanent quark confinement, *Nucl.Phys.* **B138**, 1 (1978).
- [28] G. 't Hooft, Confinement and topology in non-Abelian gauge theories, *Austriaca Suppl.* **22**, 531 (1980), <https://inspirehep.net/literature/153949>.
- [29] G. 't Hooft, Topology of the gauge condition and new confinement phases in non-Abelian gauge theories, *Nucl. Phys.* **B190**, 455 (1981).
- [30] G. 't Hooft, The topological mechanism for permanent quark confinement in a non-Abelian gauge theory, *Phys. Scr.* **25**, 133 (1982).
- [31] H. B. Nielsen and P. Olesen, A quantum liquid model for the QCD vacuum: Gauge and rotational invariance of domain and quantized homogeneous color fields, *Nucl. Phys.* **B160**, 380 (1979).
- [32] J. Ambjorn and P. Olesen, On the formation of a random color magnetic quantum liquid in QCD, *Nucl. Phys.* **B170**, 60 (1980).
- [33] G. Mack, Predictions of a Theory of Quark Confinement, *Phys. Rev. Lett.* **45**, 1378 (1980).
- [34] G. Mack and V.B. Petkova, Sufficient condition for confinement of static quarks by a vortex condensation mechanism, *Ann. Phys. (N. Y.)* **125**, 117 (1980).
- [35] J. M. Cornwall, Quark confinement and vortices in massive gauge invariant QCD, *Nucl. Phys.* **B157**, 392 (1979).
- [36] K. Langfeld, O. Tennert, M. Engelhardt, and H. Reinhardt, Center vortices of Yang-Mills theory at finite temperatures, *Phys. Lett. B* **452**, 301 (1999).
- [37] M. Engelhardt, K. Langfeld, H. Reinhardt, and O. Tennert, Deconfinement in $SU(2)$ Yang-Mills theory as a center vortex percolation transition, *Phys. Rev. D* **61**, 054504 (2000).
- [38] J. Gattnar, K. Langfeld, and H. Reinhardt, Center-vortex dominance after dimensional reduction of $SU(2)$ lattice gauge theory, *Phys. Lett. B* **489**, 251 (2000).
- [39] M. Engelhardt and H. Reinhardt, Center projection vortices in continuum Yang-Mills theory, *Nucl. Phys.* **B567**, 249 (2000).
- [40] T. Suzuki, A new scheme for color confinement due to violation of the non-Abelian Bianchi identities, *Phys. Rev. D* **97**, 034501 (2018).
- [41] H. Reinhardt and M. Engelhardt, *Center Vortices in Continuum Yang-Mills Theory* (World Scientific- Co. Pte. Ltd, Singapore, 2001).
- [42] E. Witten, The $1/N$ expansion in atomic and particle physics, in *Recent Developments in Gauge Theories*, 1979 Cargese Summer Inst., edited by 't Hooft, *et al.* (Plenum, New York, 1980), pp.403–420.
- [43] J. Greensite and M.B. Halpern, Suppression of color screening at large N , *Phys. Rev. D* **27**, 2545 (1983).

- [44] K.-I. Kondo, Magnetic monopoles and center vortices as gauge-invariant topological defects simultaneously responsible for confinement, *J. Phys. G* **35**, 085001 (2008).
- [45] S. M. Hosseini Nejad and S. Deldar, Contributions of the center vortices and vacuum domain in potentials between static sources, *J. High Energy Phys.* **03** (2015) 016.
- [46] S. Deldar, Static SU(3) potentials for sources in various representations, *Phys. Rev. D* **62** 034509 (2000).
- [47] G. Bali, Casimir scaling of SU(3) static potentials, *Phys. Rev. D* **62** 114503 (2000).
- [48] L. D. Debbio, M. Faber, J. Greensite, and S. Olejnik, Center dominance, Casimir scaling, and confinement in lattice gauge theory, arXiv: hep-lat/9802003v1.
- [49] F. V. Gubarev, A. V. Kovalenko, M. I. Polikarpov, S. N. Syritsyn, and V. I. Zakharov, From confining fields on the lattice to higher dimensions in the continuum, *Phys. Lett. B* **574**, 136 (2003).
- [50] L. D. Debbio, M. Faber, J. Greensite, and S. Olejnik, Casimir scaling vs. Abelian dominance in QCD string formation, *Phys. Rev. D* **53**, 5891 (1996).